

Issues and applications in ultra-sensitive molecular spectroscopy

Chikako Ishibashi ^{*a}, Jun Ye ^b, and John L. Hall ^b

JILA, ^aUniversity of Colorado and ^bNational Institute of Standards and Technology

Boulder, Colorado 80309-0440

ABSTRACT

We present a systematic analysis of ultra-sensitive molecular detection methods based on an optical cavity and frequency modulation spectroscopy. Our goal is towards the improvement of the limiting attainable performance by the choice of optical configuration, sample gas pressure, laser mode size, laser intensity, and detection method was discussed. The application of sensitive detection techniques emphasized here is for laser frequency stabilization, leading to better optical frequency standards and clocks.

Keywords: cavity-enhanced spectroscopy, frequency standard

1. Introduction

Cavity enhanced spectroscopy is one of the most powerful tools for sensitive molecular detection. The long absorption length in an optical cavity helps to realize highly sensitive detection of weak molecular absorptions. Another benefit of an optical cavity is enhancement of the optical power, which is important for saturation spectroscopy of weak transitions. In 1994 de Labacherie et.al. observed the saturation spectrum C₂H₂ combination band in the 1.5 μm region.¹ Ye et.al. observed saturation absorption spectra of C₂HD and CO₂ high overtone transitions at 1064 nm,²⁻⁵ and of C₂H₂ in the 1030 nm region.⁶ The sensitivity of the cavity-enhanced spectrometer is also dramatically improved by combination with a frequency modulation technique for suppression of amplitude noise in the transmitted light.^{4,7} These techniques were also applied by Ishibashi et.al. to high resolution spectroscopy of CH₄ and CH₃I in the 1.65-1.66 μm region⁸⁻¹⁰ Recently, Ye et.al. developed a novel scheme of cavity ring-down spectroscopy using frequency switching to achieve shot-noise limited sensitivity with microwatt optical power levels.¹¹

Using these results as a guide, the purpose of this paper is to consider the choice of optical topology and of experimental parameters such as laser intensity, laser beam mode size, sample gas pressure, and detection method, all of which influence/control the attainable sensitivity. Ideally, we can identify an “optimum scheme” for a particular application.

The high sensitivity of cavity-enhanced spectroscopy is important not only for the detection of weak molecular absorptions but also for attaining highly precise laser frequency stabilization, e.g. for metrological application such as frequency standards and optically based clocks. The frequency instability of a laser locked to atomic or molecular absorption line is estimated by

$$\delta\nu = \frac{\Delta\nu}{\nu \cdot (S/N)} = \frac{1}{Q \cdot (S/N)}, \quad (1)$$

where $\Delta\nu$ is width of the absorption line, ν is the laser frequency, S/N is the signal to noise ratio of the recovered resonance information, and Q is the resonance line quality factor. Hence, both narrower absorption lines and better signal to noise ratios are helpful to improve frequency stability.

It is known that linewidth of atomic or molecular absorptions are dependent on spontaneous decay rate, sample gas pressure, transit time, optical power, and frequency spectrum of the interrogating radiation. Describing the resonance linewidth over the full range of parameters would be a daunting task: just one example is the evolution of a logarithmic singularity at line center for a free-flying quantum absorber – the so-called transit-broadened lineshape at low power. However, to improve the S/N with only modest additional broadening, one may choose to use a significant pressure, for example allowing collisions to increase, perhaps double, the absorber’s natural linewidth due to the spontaneous fluorescence, or the dimensionally defined transit linewidth of $u/(2\pi w_0)$, where u is the mean velocity of molecules and w_0 is the optical beam waist radius. Under these conditions one finds a lineshape, which is rather accurately Lorentzian,

with an essentially linear pressure broadening rate. A still richer situation is obtained when the perspectives are broadened to include choice of another size for the laser beam. Basically, the minimum pressure-broadening process includes quenching of the optical dipole moment which is the dominant process when considering a near-atmospheric pressure range. However, in our high resolution domain at much lower pressures (10^{-4} to 10^{-8} atm), the dominant pressure effects are often due to velocity-changing collisions. The saturated-absorption process provides resolution below the Doppler “limit” because the nonlinear saturation is concentrated in a narrow spectral/velocity window of width fixed by the relaxation processes. Even for molecular iodine, with its $\sim \mu\text{s}$ fluorescence decay time, we can achieve a linewidth 1000-fold smaller than the Doppler case. This corresponds to a velocity width for the saturated molecules in the range of 0.3 m/s, parallel with the optical beams. Depending on resolution employed, this velocity width will be scaled accordingly. The intermolecular forces between colliding molecules, even without resonant couplings, will have at least Van-der Waals potentials $\sim R^{-6}$, leading to an intermolecular force R^{-7} . During the collision, some momentum will be transferred, leading to a new axial velocity afterward. Some geometrical issues were worked out by Hall.¹⁴ Additionally, in the case where our transition involves an electronically excited state, we can expect some important differences in the collision potentials between ground and excited states. In this case, during the collision, the ground and excited states of the coherent wavefunction will have phase evolutions at different rates, leading to a phase shift of the optical dipole by the collision. This is just one of the processes that would appear as a “dephasing” or T_2 process in our resonance description. Thus the apparent pressure-broadening rate is expected to be resolution-dependent since even a tiny velocity shift will remove a particle from the velocity-resonant packet if the spectral/velocity resolution is high. Studies at varying sub-Doppler resolutions on the P(7) line in the CH_4 rotation-vibration ν_3 -fundamental band at 3392 nm showed an increased broadening rate with resolution, relative to the low-resolution (Doppler-broadened) limit.¹⁵

For a homogeneously broadened line, one expects a “power-broadening” linear in the applied radiation’s intensity. Of course, in the gas phase where all velocities are present, one will have the inhomogeneous broadening case where the broadening of a single velocity packet is partially masked by the fact that the higher intensity can at least partially “talk to” the somewhat non-resonant velocity neighbors. This inhomogeneous broadening limit $\Delta\nu$ is described by the compounding of natural linewidth Γ_n , transit time broadening Γ_t , pressure broadening Γ_p , and laser linewidth Γ_l as

$$\Delta\nu = \left(\Gamma_n + \Gamma_t + \Gamma_p + \Gamma_l \right) \sqrt{1 + S}, \quad (2)$$

where S is the ratio (I/I_s) of laser power I , to the absorber’s saturation power I_s , and is called the saturation parameter. Therefore to obtain a narrow spectrum, a low pressure and a low saturation parameter are required. However, because the signal size of the saturation absorption signal is proportional to sample gas pressure, obtaining a high S/N is difficult with low sample pressure and so highly sensitive detection is necessary.

From the point of view of metrological applications, the use of a low pressure sample is additionally important for minimizing the collision-induced pressure *shift* and reducing the influence on the baseline by the linear Doppler background. Additionally the compactness of a spectrometer is important in the application of frequency standards to achieve high temperature stability and convenience. In this case, a cavity enhanced spectrometer design is again useful to obtain high S/N with a short cell while avoiding degradation of accuracy and/or reproducibility due to the wave front distortion of laser beam, since an optical cavity also functions as a good spatial mode selector.

We next consider optimizing the spectrometer design for a highly stable and reproducible frequency standard using a cavity enhanced spectrometer for stabilization of a 1.064 μm solid state Nd:YAG laser to an I_2 absorption line.

2. Design of spectrometer

2.1 Laser source and absorber gas for optical frequency standards

To design a sensitive spectrometer for precise laser frequency control, we have first to choose the sample gas, spectral region, and laser source. One can expect a much higher Q value, i.e. higher frequency stability, for frequency standards in the optical region than for frequency standards or clocks established in radio frequency or microwave regions. This issue has been studied actively and widely using lasers with high frequency stability. In the infrared region, there are many strong molecular ro-vibrational transitions which are good frequency references. For example, frequency coincidence of the He-Ne laser with CH_4 absorptions at a wavelength of 3.39 μm or the CO_2 laser with OsO_4 at a wavelength of 10 μm absorptions gives frequency stability of a few 100 Hz and better.

Recently, diode pumped solid state lasers were developed which can provide high frequency stability, even under free running conditions. Our work is based on a diode pumped Nd-doped YAG (Nd:YAG) laser which operates as a non-planar ring oscillator (NPRO) at a wavelength of 1064 nm. This commercial system has a frequency stability of about 5 kHz at 1 ms, which corresponds to $\sim 1.6 \times 10^{-11}$ at 1 ms. This FM noise would seriously degrade the high S/N resonances we are expecting, if a 1 ms signal sampling time were used. Clearly, to achieve, let's say 1×10^{-14} at 1 s, a 50-fold better performance of the utilized source laser is necessary. This can be accomplished in two steps. First we could modulate much more quickly, ~ 100 kHz, and so many signal samples can be acquired within the ~ 100 μ s half-period of the disturbances that lead to the NPRO's linewidth. If the molecular frequency discriminator has sufficient S/N , we can guide the laser source such that its frequency excursion is strongly reduced. Consequently the optical phase does not depart by 1 radian from our "ideal" sine wave, so the Bessel phase modulation index is very small and we have little carrier power scattered into these high frequency sidebands. A little sideband power may remain at high Fourier offset frequencies, but perhaps 99 % of the power will remain in the bright line we identify as the (nearly) sine-wave carrier. The good stability of the Nd:YAG laser as a laser source, its high power, and the strong iodine absorption matching frequency-doubled output of the laser near 532 nm are attractive and in this paper we consider the attainable frequency stability using such molecular absorption lines as frequency references. The second question is whether the resonance S/N performance will be sufficient: will we need to use a cavity resonator to obtain the high stability at short time, then use the molecular resonance to suppress drift and vibration noise from the cavity?

To be specific, after frequency doubling the 1064 nm Nd:YAG laser, as frequency references we use I_2 electronic transitions near 532 nm. The a_{10} hyperfine component of the R(56) 32-0 band is a typical example. The transition dipole moments are in a nice range, so that a line width of <1 MHz can result, including natural, pressure and intensity broadening. A measured S/N of 120 in a 10 kHz bandwidth has been achieved. Expressing the frequency instability with Eq (1), $\Delta\nu/(S/N)$, we expect approximately 8 kHz FM noise. The majority of the bandwidth which contributes to the noise is the last octave, so we may take the frequency rate of the noise process to be also ~ 8 kHz. This leads to a phase modulation index of $\sim >1$, and consequently considerable power is lost into noise sidebands near this frequency. If we express the measurement bandwidth instead as 0.16 Hz, corresponding to an averaging time of 1 s, the S/N is improved by a factor of $\sqrt{60,000} \sim 250$. Now the FM deviations are held to $8 \text{ kHz}/250 \sim 30$ Hz. The Allan deviation of the beat note between two I_2 -stabilized lasers was obtained as $5 \times 10^{-14}/\sqrt{\tau}$, with the integration time τ expressed in s. This is a very strong indication that we need another factor of 25 in S/N to reach the sub- 10^{-14} stability domain. Alternatively, a cavity may be used to narrow the line by pre-stabilization. However, it cannot be used to attain better long-term performance than the molecular reference signal can provide. If a S/N increase by a factor of 3 is possible, the phase modulation index would be reduced accordingly and our stabilized source would change its linewidth from ~ 8 kHz down to just a few hundred Hz!

Another candidate for frequency references in the 1064 nm region is a rotation-vibration combination band of C_2HD ($\nu_1 + 3\nu_3$). Although this transition is extremely weak, previous work using a high finesse cavity and the frequency modulation technique called NICE-OHMS (noise immune cavity enhanced optical heterodyne molecular spectroscopy) realized the observation of molecular spectra with S/N of 7670 at a time constant of 1 s and linewidth of 500 kHz (HWHM) with a 0.20 Pa sample gas pressure.³ The laser frequency was stabilized to the P(5) transition, and the beat note frequency between I_2 stabilized Nd:YAG laser showed Allan deviation of $2.0 \times 10^{-13}/\sqrt{\tau}$.

Upon, comparing the I_2 and C_2HD transitions, it is incredible that performance separated by only a factor of 4 can be obtained from absorbers with an absorption coefficient ratio of 500,000! For simplicity at least, we therefore conclude that the I_2 -stabilized Nd:YAG laser is the better candidate for an optical frequency standard. However, it does make us think that some work on S/N for the I_2 system could buy us a big return in frequency stability. In the following sections, we will discuss the optimum conditions for obtaining the largest $(S/N)/\Delta\nu$ with this system.

2.2 Detection method of molecular absorptions

To observe atomic or molecular saturated absorption spectra with high sensitivity, a long absorption length and adequate laser power are required. In the previous work of I_2 stabilized Nd:YAG laser, a 1.2-m long sample cell and 1.0 mW-pump and 0.26 mW-probe laser power were used. Although this system supplies a near-adequate S/N , the length of the cell degrades its temperature stabilization, which may cause signal size, line center frequency, and linewidth variations. With a well-stabilized sidearm temperature to fix the vapor pressure, in principle changes would occur only via the second-order Doppler effect. However, one finds a strong two-time-constant behavior after a step change of sidearm

temperature, due to a storage effect by residual binding of the I_2 molecules to the glass wall of the cell. Thus room temperature changes can temporarily change the iodine pressure.

A compact geometry with good thermal control possibilities could be provided by a multi-pass cell to supply a long absorption length that helps to maintain/increase the S/N . Disadvantages of the multi-pass cell are that optical alignment can be difficult. Additionally one should be careful to avoid interference effects which cause undesirable interference fringes in the signal.

An optical cavity is useful to make the spectrometer compact but yet with enhanced absorption length, i.e. high S/N . A cavity also works as a spatial mode selector of the input laser beam, which results in a better defined Gaussian mode inside the cavity and contributes to reliable reproducibility as mentioned in the section 2.4. In this paper, we consider the optimum design of a cavity-enhanced spectrometer.

Another important issue for design the spectrometer is the detection scheme. The frequency modulation (FM) technique is one of the best ways to avoid low frequency noise and to achieve shot-noise limited sensitivity. For laser frequency stabilization, the dispersion lineshape signal obtained with FM spectroscopy is used as the frequency discrimination signal for frequency locking. However when one uses a cavity as an absorption cell, there are some difficulties using the FM technique because a cavity also works as a frequency discriminator, which may add noise. Additionally, the modulation frequency is limited by the cavity response time.

Cavity dithering is often used to avoid this difficulty and to apply phase modulation to the optical field inside the cavity. Usually the modulation frequency of cavity dither is relatively low, say up to a few hundred kHz, because it is limited by the cavity mirror's mechanical response time. And the transmitted radiation possibly contains amplitude modulation due to the imperfection of frequency stabilization to the cavity.

Another scheme is to choose the modulation frequency f_m to match the cavity free spectral range ($f_m = \text{FSR} = c/2L$, c ; speed of light, L ; length of Fabry-Perot cavity). This method is called NICE-OHMS and is a powerful tool to utilize high frequency modulation to avoid low frequency noise. One “feature” of NICE-OHMS is that two sideband-generated molecular resonance signals result at frequencies $f_m/2$ apart from the molecular center frequency. Thus one should carefully choose the modulation frequency, i.e. cavity length, to avoid being disturbed by these extra resonances when the method is applied to molecules such as I_2 that have dense spectra. See the discussion in the following section.

If it is possible to use a ring cavity, e.g. a bow-tie type cavity, the modulation transfer technique is available¹². In modulation transfer, only the pump beam is frequency modulated and a relatively weak probe beam is detected and demodulated. Because of the four wave mixing effect, modulation in the pump beam is transferred to the probe beam. This technique has only a multiplicative sensitivity to a small residual amplitude modulation, compared with the usual additive sensitivity. Consequently it is useful in determining the center frequency of a molecular absorption line.¹³

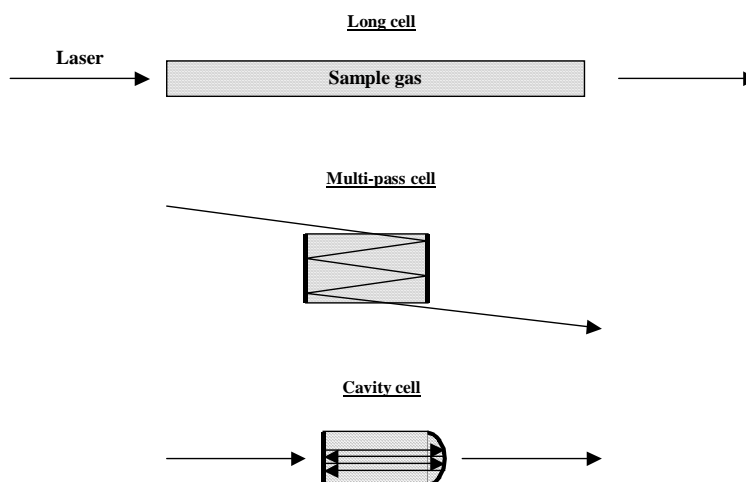


Fig. 1: Absorption cell design to enhance signal to noise ratio.

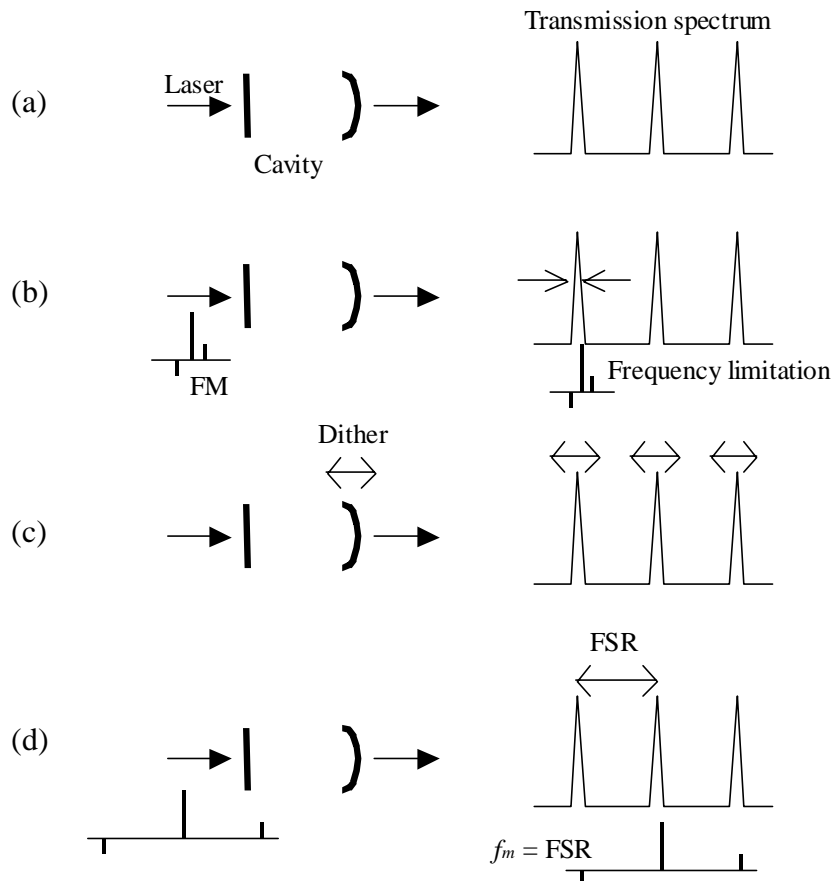


Fig. 2 Frequency modulation scheme for cavity-enhanced spectrometer.
 (a) Cavity transmission spectrum, (b) Low frequency FM, (c) Cavity dither modulation, (d) NICE-OHMS

2.3 Estimation of attainable linewidth and signal to noise ratio

In this section, we discuss optimization of several operating parameters and the performance of an iodine spectrometer. Here we assume the pump/probe configuration depicted in Fig. 3. (We have omitted some optical elements in the spectrometer such as polarizers, the AOM frequency shifter and other beam isolation elements.) Saturation parameters are defined as S_s and S_p for saturation and probe beam, respectively.

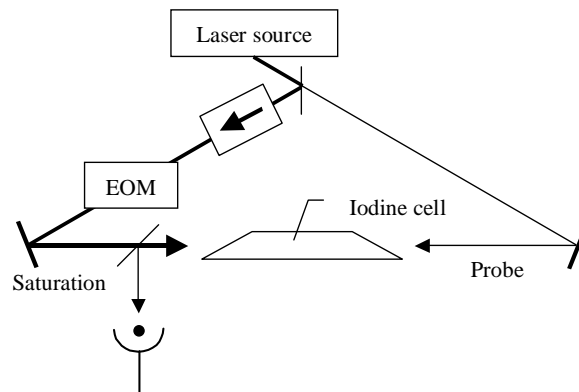


Fig. 3 Basic configuration for saturation spectroscopy.

Consider first the saturation parameter needed to obtain the maximum S/N slope. The saturation signal contrast is described as:

$$\Delta\alpha = \alpha_0 \left(\frac{1}{\sqrt{1+S_p}} - \frac{1}{\sqrt{1+S_s+S_p}} \right), \quad (3)$$

where α_0 is the linear absorption coefficient. In the standing-wave case where $S_s = S_p = S$, Eq (3) becomes

$$\Delta\alpha = \alpha_0 \left(\frac{1}{\sqrt{1+S}} - \frac{1}{\sqrt{1+2S}} \right). \quad (4)$$

The signal size is proportional to the probe beam power, and can be determined by

$$\text{Signal} \propto S_p \left(\frac{1}{\sqrt{1+S_p}} - \frac{1}{\sqrt{1+S_s+S_p}} \right). \quad (5)$$

For the two-beam-configuration saturation spectroscopy, the power broadening described in Eq (2) is rewritten as

$$\Delta\nu = (\Gamma_n + \Gamma_t + \Gamma_p + \Gamma_l) \frac{\sqrt{1+S_s} + \sqrt{1+S_p}}{2}, \quad (6)$$

If the detection sensitivity is limited by shot noise, it is represented as

$$\text{Shot} \cdot \text{noise} \propto \sqrt{S_p + N_{amp}}, \quad (7)$$

where N_{amp} is the equivalent amplifier noise of the detector. Therefore we obtain the saturation parameter-dependence of S/N slope as

$$\frac{S/N}{\Delta\nu} \propto S_p \left(\frac{1}{\sqrt{1+S_p}} - \frac{1}{\sqrt{1+S_s+S_p}} \right) \cdot \left(\frac{2}{\sqrt{1+S_s} + \sqrt{1+S_p}} \right) \cdot \frac{1}{\sqrt{S_p + N_{amp}}}. \quad (8)$$

Figure 4 shows the calculated S/N slope for $S_p/S_s = 0.25, 0.5, 1.0$. Each curve shows the maximum S/N slope value, which means the saturation parameter can be optimized to obtain maximum S/N slope value. For $S_p/S_s = 0.25, 0.5$, and 1 , the S/N -slope curve has a maximum value at $S_s = 6.2$ ($S_p = 1.6$), $S_s = 4.0$ ($S_p = 2.0$), and $S_s = 2.5$ ($S_p = 2.5$). In the rest of this paper, we will estimate the expected frequency stability for assuming $S_p/S_s = 0.5$ and $S_s \sim 2.30$ ($S_p = 1.15$), where we are sacrificing about 6 % in sensitivity to avoid unrewarded saturation broadening.

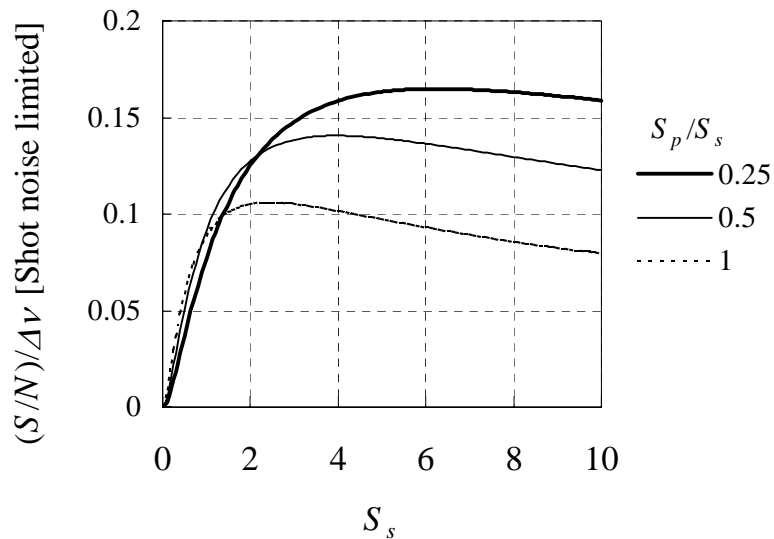


Fig. 4 Saturation-parameter dependence of S/N slope. N_{amp} was taken to 0.1.

If the absorption is large, i.e. $\alpha L > 1$, shot noise is rewritten by

$$\text{Shot} \cdot \text{noise} \propto \sqrt{S_p \cdot e^{-\alpha_s L} + N_{amp}}, \quad (9)$$

where α_s is the probe-saturated absorption coefficient described by

$$\alpha_s = \frac{\alpha_0}{\sqrt{1 + S_p}}, \quad (10)$$

Next we consider the choice of a sample gas pressure, laser beam size, optical power, and estimate the linewidth obtained with this design according to Eq (6) with experimentally obtained parameters. Although a higher pressure results in a larger signal size, the temperature dependence is also larger. As a result the I₂ reservoir requires better temperature stability to avoid frequency variations caused by the pressure shift. For example, the temperature-dependent pressure slope at 1 °C is 0.45 Pa/°C.¹⁶ Considering this with the pressure shift of -3.2 kHz/Pa,¹⁷ a temperature dependence of absorption frequency shift is obtained as -1.44 kHz/°C. To obtain 1-Hz frequency stability, the system needs <1 m°C temperature stability, which begins to be difficult to achieve for long term. Therefore, a lower pressure region may be more suitable for the frequency standards. For example, at 0.5 Pa (-18 °C), the temperature dependent frequency shift is estimated as -220 Hz/°C. The low pressure sample gas is also useful to reduce pressure broadening. Of course, there is a trade-off between long-term frequency shifts at elevated pressures and reduced signal absorption at low pressure.

To estimate the expected frequency stability of the laser, first, we will estimate the operating linewidth $\Delta\nu$. Based on measurements at JILA, the natural broadening for iodine 532 nm transitions may be taken as 220 kHz, while the pressure broadening (also HWHM basis) is approximately

$$\Gamma_p = 120 \text{ kHz/Pa} \times P. \quad (11)$$

At a pressure of 0.5 Pa, this contribution is 60 kHz. Transit time broadening for I₂ molecule is estimated using a probable thermal velocity of 140 m/s at a room temperature as

$$\Gamma_t = 22 \text{ kHz} \cdot \text{mm} / w_0, \quad (12)$$

where w_0 is the laser beam radius. The laser beam diameter $2w_0$ is ~ 1 mm, which gives the transit time broadening of $\Gamma_t \sim 44$ kHz. The typical Nd:YAG laser has linewidth of $\Gamma_l = 5$ kHz. From Eq (6), the total linewidth $\Delta\nu$ of the saturated absorption resonance at saturation parameters $S_s = 2.30$ and $S_p = 1.15$ is estimated to be 540 kHz.

Now we move to the estimation of S/N . The measured unsaturated absorption for iodine is $\sim 0.0013 \text{ cm}^{-1}/\text{Pa}$ for an individual hyperfine component near Doppler line center of the R(56) 32-0 band. With our adopted saturation parameter of $S_s = 2.30$ and $S_p = 1.15$, from Eq (3) we can expect a resonant saturated-absorption peak contrast of 21 % of the single line absorption, i.e. $2.7 \times 10^{-4} \text{ cm}^{-1}/\text{Pa}$. Additional hyperfine components contribute saturable opacity, combining to $\sim 0.0106 \text{ cm}^{-1}/\text{Pa}$ when their Doppler frequency offsets are considered. Of course this is non-resonant opacity, but it is suppressed by $(2.15)^{1/2}$ according to the saturation effect written by Eq (10). Thus the single beam's saturation reduces the Doppler summed opacity to $0.007 \text{ cm}^{-1}/\text{Pa}$.

As a concrete case, consider the use of Brewster-window iodine cells with a 10-cm active length and a 12-cm tip-tip length. At 0.5 Pa, the signal opacity is 1.35×10^{-3} and the background single-pass absorption is 3.6 %. Let's start without a cavity. The saturation power for a $2w_0 = 1$ mm beam would be ~ 0.45 mW at the assumed 0.5 Pa. The adopted 2.30 and 1.15 saturation factors leads to input powers of 1.0 and 0.52 mW for saturation and probe. The expected signal is 0.7 μW in the transmitted background optical power of 0.50 mW, leading to a shot-noise limited S/N estimated as 8×10^4 at 1 s using the equation of

$$S/N = \sqrt{\frac{\eta}{2eB}} \cdot \frac{P_{sig}}{\sqrt{P_{background}}}, \quad (13)$$

where η is the responsivity of the detector, e is the electron charge, B is the detection bandwidth, and P_{sig} and $P_{background}$ are optical powers of signal and background, respectively. Here we used the values of $B = 1/2\pi \text{ Hz}$ (for 1 s averaging time), $\eta = 0.33 \text{ A/W}$. If $P_{sig} = P_p \Delta\alpha L$ and $P_{background} = P_p \exp(-\alpha_s L) \sim P_p$, then Eq (13) is rewritten by

$$S/N = \sqrt{\frac{\eta}{2eB}} \cdot \Delta\alpha L \sqrt{P_p}. \quad (14)$$

Using FM spectroscopy to minimize technical noise, the signal size is determined by the beat note power, so the frequency instability is rewritten as

$$\delta\nu = \frac{\Delta\nu}{\nu \cdot (S/N)} \cdot \frac{1}{J_0(\beta)J_1(\beta)}, \quad (15)$$

where $J_n(\beta)$ is n -th order Bessel function. $J_0(\beta)J_1(\beta)$ has the maximum value of 0.339 at $\beta = 1.08$. The projected frequency instability would then be 3.4×10^{-14} . (Roughly speaking, this just about matches our experience, BUT we used a cell about 12-fold longer. So it is quite likely another important noise source is present - which is most likely the fast frequency noise of the NPRO source).

Next we consider the desirable cell length and cavity design to enhance S/N . We suppose a bow-tie cavity configuration of about 50 cm length as shown in Fig. 5. The cavity finesse is given by

$$F = \frac{\pi}{T + l + \alpha L_{cell}}, \quad (16)$$

where T is the transmittance of the coupling mirror, l is the total loss of the cavity mirrors and cell window, and αL_{cell} is the one pass absorption by iodine molecules. As mentioned above, we suppose αL_{cell} is 3.6 % (I_2 pressure 1.0 Pa, $L_{cell} = 10$ cm). If l is 1 %, the total loss of light with one pass of the cavity is about 4.6 %. We consider the case that the mirror transmittance T is almost the same as the one-pass loss, then $F \sim 35$. The effective optical pass length is enhanced in the cavity by a factor of $2F/\pi$, which is estimated as 22 for $F = 35$ cavity. Optical power is also enhanced in the cavity, which

is expressed by $\frac{F}{\pi} \cdot \frac{T}{T + l + \alpha L_{cell}}$. As mentioned above, if we suppose $T = \alpha L_{cell} + l$, the factor is $F/2\pi$. The input

laser power should be reduced to keep the preferable saturation inside the cavity, so as not to decrease the signal size. For the shot-noise limited detection, the S/N decreases due to the power reduction by a factor of $(2\pi/F)^{1/2}$, which is calculated as 0.42 for $F = 35$. Hence the total S/N increases by a factor of

$$F_{S/N} = 2\sqrt{\frac{2F}{\pi}} \quad (17)$$

and is estimated as 9.4 for $F = 35$ cavity. The frequency stability expected for the cell spectrometer is then re-estimated as $3.6 \times 10^{-15}/\sqrt{f}$, which is one order better than the previous experiment. As cavity parameters, we can expect, for example, $L_{cav} = 50$ cm, FSR = 600 MHz, and cavity fringe width of 17 MHz (FWHM).

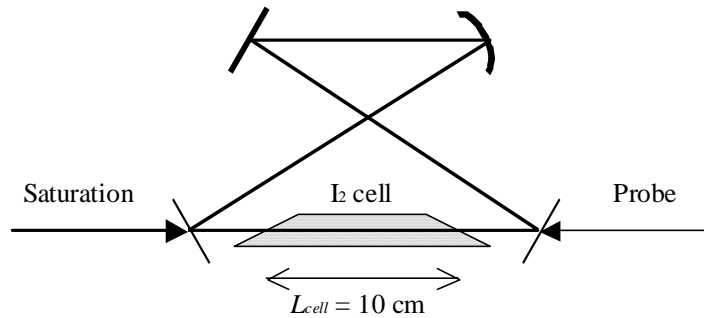


Fig. 5 Bow-tie cavity spectrometer for saturation spectroscopy of iodine.

This moderate finesse bow-tie cavity cell design has several advantages. First the spectrometer size is compact, and high temperature stabilization can be expected. Second, saturation and probe beams can be separated, because of the running-wave configuration of the cavity, which results in better signal contrast than in the equal power configuration. Third, FM spectroscopy is available with this spectrometer because of the broad cavity transmittance spectra. Finally, the cavity works as a spatial mode selector of the laser beam, hence we can expect good alignment reproducibility even with a compact system. The mode waist size $2w_0 = 1$ mm is feasibly attained using an $R = 10$ m mirror. Importantly, the NICE-OHMS method is also available for this cavity spectrometer if the FSR is set near 540 MHz. The 540-MHz sidebands in this case fall nicely into open places in the I_2 spectrum so there will be no undesired unbalance of the

NICE-OHMS FM spectrum, as would be caused by “main” lines or cross-over resonances. Also the FM spectroscopy approach is sensitive to spectral components offset by $\frac{1}{2}$ the modulation frequency, due to Doppler-generating crossover resonances, so we also have to avoid these side-band generated spectra. Amazingly for such a complex spectrum¹⁸, it appears that a cavity length of 55.5 cm ($c/L = 540$ MHz) should provide an interference-free operation.

2.4 Accuracy and reproducibility of spectra

Although previous optical frequency standards have high stability in short term (< 100 s), the long term stability and reproducibility are still problematic.

Temperature variations in the sample gas reservoir cause frequency instability especially in case of iodine because it changes the iodine pressure, leading to frequency shift. At the iodine operating temperature about -18°C (vapor pressure of 0.5 Pa), the temperature dependence of iodine pressure is ~ 0.07 Pa/ $^\circ\text{C}$. For example sidearm (reservoir) the temperature variation easily can be suppressed less than 5 m $^\circ\text{C}$, and so the pressure shift caused by temperature fluctuation is less than ~ 1.1 Hz. However, as noted above, temperature changes of the cell walls give rise to rather large – if temporary – pressure changes.

Residual amplitude modulation (RAM) in a frequency modulation system is an important issue for the discussion of the accuracy and reproducibility of optical frequency standards. RAM levels can easily approach the percent domain and seriously degrade the sensitivity and distort the spectral shape in the FM spectroscopy. In this new epoch when optical frequencies can be easily and accurately measured, RAM also gives undesirable offsets and noise in error signals for laser frequency stabilization, causing frequency offsets from the center of the frequency reference and aggravating the instability problems, particularly at long times since RAM amplitude is sensitive to crystal temperature change or electric field inhomogeneity. Experimental measurement showed that, with some care, a stable RAM level of 2.3 ppm can be obtained directly using an ADP crystal at a modulation frequency of 220 kHz. Even this RAM level still gives noticeable frequency offset from the center frequency of frequency references (molecular absorption lines). For example, in an I_2 spectrum with a linewidth of 540 kHz, this RAM causes about 1 Hz frequency offset with modulation transfer, and 10-100-fold more with simple FM detection. Though this offset frequency does not degrade the reproducibility as long as it is stable, it is better to suppress/stabilize RAM with an active feedback system.

Alignment stability and reproducibility is also important for the reproducibility of the optical clock because wave front distortion of a laser beam will also cause a frequency offset. Especially a compact spectrometer system tends to have a low reproducibility of running-wave alignment because of the short optical path length. Again a cavity, which works as a mode selector for the laser beams, is useful to increase reliability of alignment reproducibility. We believe the cavity spectrometer system should have the same - or superior - reproducibility as the previous system using a long I_2 cell.¹⁹

Therefore, the irreproducibility of this cavity spectrometer should be < 5 Hz. This projected cavity-based system is under construction at JILA.

2.5 Other example designs

Here we consider some other candidates for optical frequency standards and the spectrometer design. The example calculation results are summarized in Table 1.

The Yb:YAG laser (which supplies 1030 nm radiation) also has stable and narrow frequency performance, and hence can be a candidate for frequency standard. There is an acetylene vibrational overtone band at the laser’s wavelength and iodine bands in the second harmonic region. Though the acetylene overtone transition is very weak, it has been shown that a high finesse cavity spectrometer and NICE-OHMS technique can attain high sensitivity. In the previous experiment with a 75,000 finesse Fabry-Perot cavity cell, the sensitivity of 7×10^{-11} was obtained with acetylene (C_2H_2).⁶ The absorption coefficient has been experimentally obtained as 3.2×10^{-8} cm⁻¹/Pa. For the R(29) transition, the saturation power density is $I_s = 20$ W/mm² with about 1.3-Pa pressure. According to Eq (8), the S/N slope has maximum value at $S = 2.5$ for the Fabry-Perot cavity configuration ($S_s = S_p = S$). If we suppose the Fabry-Perot cavity has a beam waist of 410 μm , to obtain $S = 2.5$ the optical power needed is estimated as 13 W. Here we suppose the $S = 1$, i.e. -an optical power of 5.2 W inside the cavity though the expected S/N slope is factor of 0.84 smaller than the maximum value. In the case of molecular overtones, the minimum absorption linewidth is primarily determined by the transit time broadening: $\Gamma_t = 135$ kHz for 410 μm beam size. Pressure broadening is estimated as 110 kHz at 1 Pa. Then the total

linewidth including the saturation effect is estimated as 310 kHz. Suppose the cavity finesse and transmission efficiency are 75,000 and 20 %, input and output optical power should be 0.90 mW and 0.18 mW to obtain 5.2 W inside the cavity. Using these parameters, shot-noise limited S/N is estimated as 5.0×10^5 at 1 s, which gives the expected frequency stability of $6.5 \times 10^{-15}/\sqrt{F}$.

Previous study of the I_2 spectral width around the 515 nm region showed narrower natural broadening than in the 532 nm region,^{20,21} and recently precise study of the natural broadening of I_2 spectra at 489-532 nm revealed $\Gamma_n \sim 50$ kHz at 516 nm,²² which is 4.4 times narrower than that at the wavelength region of 532 nm. Therefore if the same spectrometer designed for 532 nm iodine spectrometer is applied to 516 nm system, we can expect 4.4 times better frequency stability.

Table 1. Spectrometer design and expected frequency stability.

Molecule	Wavelength (Laser)	Transition	α_0	L_{cav} & F	Instability
I_2	532 nm (SHG of Nd:YAG)	X-B, R(56) 32-0	$1.3 \times 10^{-3} \text{ cm}^{-1}/\text{Pa}$	50 cm, 35	$3.6 \times 10^{-15}/\sqrt{F}$
C_2H_2	1031 nm (Yb:YAG)	$3\nu_3$, R(29)	$3.2 \times 10^{-8} \text{ cm}^{-1}/\text{Pa}$	50 cm, 75000	$6.5 \times 10^{-15}/\sqrt{F}$
I_2	515 nm (SHG of Yb:YAG)	X-B, P(61) 43-0	$6 \times 10^{-4} \text{ cm}^{-1}/\text{Pa}$	50 cm, 70	$8.2 \times 10^{-16}/\sqrt{F}$

3. Conclusion

We discussed detailed spectrometer design issues relative to increasing the performance of a laser frequency stabilization system. The optimum condition of saturation parameter to obtain the best $(S/N)/\Delta\nu$ was discussed. A cavity-based approach seems desirable for the best performance and, with a cavity finesse of 35, the expected frequency stability of Nd:YAG laser stabilized to 532 nm iodine transition was estimated as $3.6 \times 10^{-15}/\sqrt{F}$. Reproducibility of this spectrometer is expected to be less than 5 Hz. To realize this performance, the probe laser frequency stability will be required to be improved.

Acknowledgement

We are grateful to W.-Y. Cheng and L.-S. Chen for fruitful discussions about their experimental results of iodine spectra at 516 nm. Professor L.-S. Ma is thanked for his many contributions to this work in its earlier stages. This research is supported in part by NASA and by NSF, while NIST provides continuing support for research in the possible new realizations of the fundamental standards.

References

1. M. de Labacherie, K. Nakagawa, and M. Ohtsu, "Ultra-narrow $^{13}C_2H_2$ saturated-absorption lines at 1.5 μm ," *Opt. Lett.* **19**, pp. 840-842, 1994.
2. L.-S. Ma, J. Ye, P. Dubé, and J. L. Hall, *Laser Spectroscopy XII*, World Scientific, Singapore, 1996.
3. J. Ye, L.-S. Ma, and J. L. Hall, "Sub-Doppler optical frequency reference at 1.064 μm by means of ultrasensitive cavity-enhanced frequency modulation spectroscopy of a C_2HD overtone transition," *Opt. Lett.* **21**, pp. 1000-1002, 1996.
4. J. Ye, L.-S. Ma, and J. L. Hall, "Ultrasensitive detections in atomic and molecular physics – demonstration in molecular overtone spectroscopy," *J. Opt. Soc. Am.* **B 15**, pp. 6-15, 1998.
5. J. Ye, L.-S. Ma, and J. L. Hall, "Ultrastable optical frequency reference at 1.064 μm using a C_2HD molecular overtone transition," *IEEE Trans. Instrum. Meas.* **46**, pp. 178-183, 1997.

6. J. Ye, L.-S. Ma, and J. Hall, "High-resolution frequency standard at 1030 nm for Yb:YAG solid-state laser," *J. Opt. Soc. Am. B* **17**, pp. 927-931, 2000.
7. L.-S. Ma, J. Ye, P. Dubé, and J. L. Hall, "Ultrasensitive frequency-modulation spectroscopy enhanced by a high-finesse optical cavity: theory and application to overtone transitions of C₂H₂ and C₂HD," *J. Opt. Soc. Am. B* **16**, pp. 2255-2268, 1999.
8. H. Sasada, K. Suzumura, and C. Ishibashi, "Coriolis-dependent Stark effect of the 2ν₃ band of methane observed by saturated absorption spectroscopy," *J. Chem. Phys.* **105**, pp. 9027-9034, 1996.
9. C. Ishibashi and H. Sasada, "Near-infrared laser spectrometer with sub-Doppler resolution, high sensitivity, and wide tenability: A case study in the 1.65-μm region of CH₃I spectrum," *J. Mol. Spectrosc.* **200**, pp. 147-149, 2000.
10. C. Ishibashi, R. Saneto, and H. Sasada, "Infrared radio-frequency double-resonance spectroscopy of molecular vibrational-overtone bands using a Fabry-Perot cavity-absorption cell," *J. Opt. Soc. Am. B* **18**, pp. 1019-1030, 2001.
11. J. Ye and J. L. Hall, "Cavity ringdown heterodyne spectroscopy: High sensitivity with microwatt light power," *Phys. Rev. A* **6106**, pp. 1802-1805, 2000.
12. L.-S. Ma and J. L. Hall, "Optical heterodyne spectroscopy enhanced by an external optical cavity: Toward improved working standards," *IEEE Quant. Electr.* **26**, pp. 2006-2012, 1990.
13. M. L. Eickhoff and J. L. Hall, "Optical frequency standard at 532 nm," *IEEE Trans. Instrum. Meas.* **44**, pp. 155-158, 1995.
14. J. L. Hall, "The lineshape problem in laser-saturated molecular absorption," In lectures in theoretical physics XII, pp. 161-210, 1973.
15. R. L. Barger and J. L. Hall, "Wavelength of the 3.39-micron laser-saturated absorption line of methane," *Appl. Phys. Lett.* **22**, pp. 196-199, 1973.
16. W. R. C. Rowley, "Frequency dependence of a 633-nm He-Ne laser stabilized by ¹²⁷I₂ upon iodine pressure, modulation amplitude, and wall temperature," NPL Report MOM 54, 1981.
17. J. Ye, L. Robertsson, S. Picard, L.-S. Ma, and J. L. Hall, "Absolute frequency atlas of molecular I₂ lines at 532 nm," *IEEE Trans. Instrum. Meas.* **48**, pp. 544-549, 1999.
18. F.-L. Hong, J. Ye, L.-S. Ma, S. Picard, C. Bordé, and J. L. Hall, "Rotation dependence of electric quadrupole hyperfine interaction in the ground state of molecular iodine by high-resolution laser spectroscopy," *J. Opt. Soc. Am. B* **18**, pp. 379-387, 2001.
19. J. Ye, L.-S. Ma, and J. L. Hall, "Molecular iodine clock," *Phys. Rev. Lett.* **87**, pp. 270801/1-4, 2001.
20. Ch. J. Bordé, G. Camy B. Decomps, and J.-P. Descoubes, "High precision saturation spectroscopy of ¹²⁷I₂ with argon lasers at 5145 Å and 5017 Å," *J. Physique*, **42**, pp. 1393-1411, 1981.
21. A. N. Goncharov, M. N. Skvortsov, and V. P. Chebotayev, "Study of relaxation of molecular-iodine by the method of saturated absorption-spectroscopy," *Appl. Phys.* **B 51**, pp. 108-115, 1990.
22. W.-Y. Cheng, L.-S. Chen, T. H. Yoon, J. L. Hall, and J. Ye, "Sub-Doppler molecular iodine transitions near the dissociation limit (523 to 498 nm)," *Opt. Lett.* **27**, pp. 571-573 (2002).